The effects of transit time heterogeneity on brain oxygenation during rest and functional activation
-
Supplementary material

Peter M Rasmussen, Sune N Jespersen, Leif Østergaard

Center of Functionally Integrative Neuroscience (CFIN), Aarhus University, Aarhus, Denmark
pmr@cfin.au.dk

Parallel changes in transit time and capillary transit time heterogeneity

There is relatively sparse literature on the extent to which the mean transit time $\bar{\tau}_c$ and the capillary transit time heterogeneity (CTH), as quantified by the standard deviation of the transit time distribution σ_c, covary. The estimates presented in Jespersen & Østergaard [1] suggest that $\bar{\tau}_c$ and σ_c may covary in the sense, that decreased heterogeneity is observed for decreased transit times. This relationship was observed in data from a series of studies, where flow was manipulated by electrical stimulation [2, 3] by lowering blood oxygen content (hypoxemia) [4, 5] and by elevating blood carbon dioxide content (hypercapnia) [5, 6].

To further explore the covariation between $\bar{\tau}_c$ and σ_c we conducted a simple simulation experiment based on a vascular anatomical network (VAN) model [7]. The VAN model provides a simplified representation of the vascular topology; the microcirculation is modelled as a branching network starting at a single feeding arteriole that, through a series of arterioles, branches into 64 capillaries and finally converges through venoules into a single draining venule. The model is based on physically measurable parameters, e.g. the resistance of individual vessel segments is modelled in terms of diameter, length, and apparent viscosity with numerical values corresponding to reports found in the literature. The VAN model accurately predicted blood pressure and hemoglobin oxygen saturation at different branch levels throughout the network despite the simplicity of the model [7]. Identical transit times are observed across all vessel segments at a specific branch order in the VAN model, e.g. all 64 capillary segments have same transit time. This lack of heterogeneity is partially due to the symmetrical topology of the network and partially due to all vessel segments at a specific branch order have identical resistance. To introduce CTH into the VAN model we follow a simple approach. In this approach we do not attempt accurately to model the *mechanism* underlying CTH. Rather a simple modification is introduced of which the *effect* is that CTH occurs in the network. Specifically, CTH was introduced as follows. In the basic form all capillary segments of the VAN model have a resistance of $r_c = 3.9 \cdot 10^{10}$ mmHg·s/l. Instead of identical resistances we now let the individual capillary resistances be distributed uniformly centred at r_c. This modification results in presence of flow heterogeneity throughout the entire network. The study of Jespersen & Østergaard [1] compiled a table with estimates of σ_c based on experimental data (Table 1 in their paper). For the two data set using electrical stimulation we computed the coefficient of variation ($\sigma_c/\bar{\tau}_c$) corresponding to baseline conditions. This coefficient was then averaged across the two data sets giving $\sigma_c/\bar{\tau}_c = 0.78$. The width of the resistance distribution, centred at r_c, was then adjusted such that the transit time coefficient of variation $\sigma_c/\bar{\tau}_c$ observed in the modified VAN model approximated 0.78.

Following this modification of capillary resistances the vessel segments in the arteriolar part of the network were dilated in order to increase flow through the network. The arteriolar vessel volumes were increased from baseline values up to values that result in a relative flow increase of around 50%, similar to flow increases observed in functional activation [3, 8].

The total flow increased from a flow of ~ 10 nl/s to ~ 15 nl/s. Figure 1 shows traces of individual capillaries (thin gray curves) while thick dashed curves show the means across the 64 capillaries over the range of changes in total flow. Figure 2 shows traces of averages and standard deviations (both flow weighted) of capillary transit times and capillary velocities over the range of changes in total flow. Flow weighted quantities were computed as follows. We let f_i denote the flow through the i'th capillary and let the weight $w_i = f_i / \sum_{i'} f_{i'}$, $i' \in \{1, 2, \ldots, 64\}$ quantify the fractional flow through the i'th capillary. Let

τ_i denote the transit time of the i'th capillary. The average of transit time and the standard deviation of transit times are computed as flow weighted quantities, with the average defined by

$$\bar{\tau}_{\mathrm{c}} = \sum_i w_i \tau_i, \tag{1}$$

and the standard deviation defined by

$$\sigma_c = \sqrt{\frac{N}{N-1} \sum_i w_i \left(\tau_i - \bar{\tau}_{\mathrm{c}}\right)^2}, \tag{2}$$

with N being the number of non-zero weights w_i.

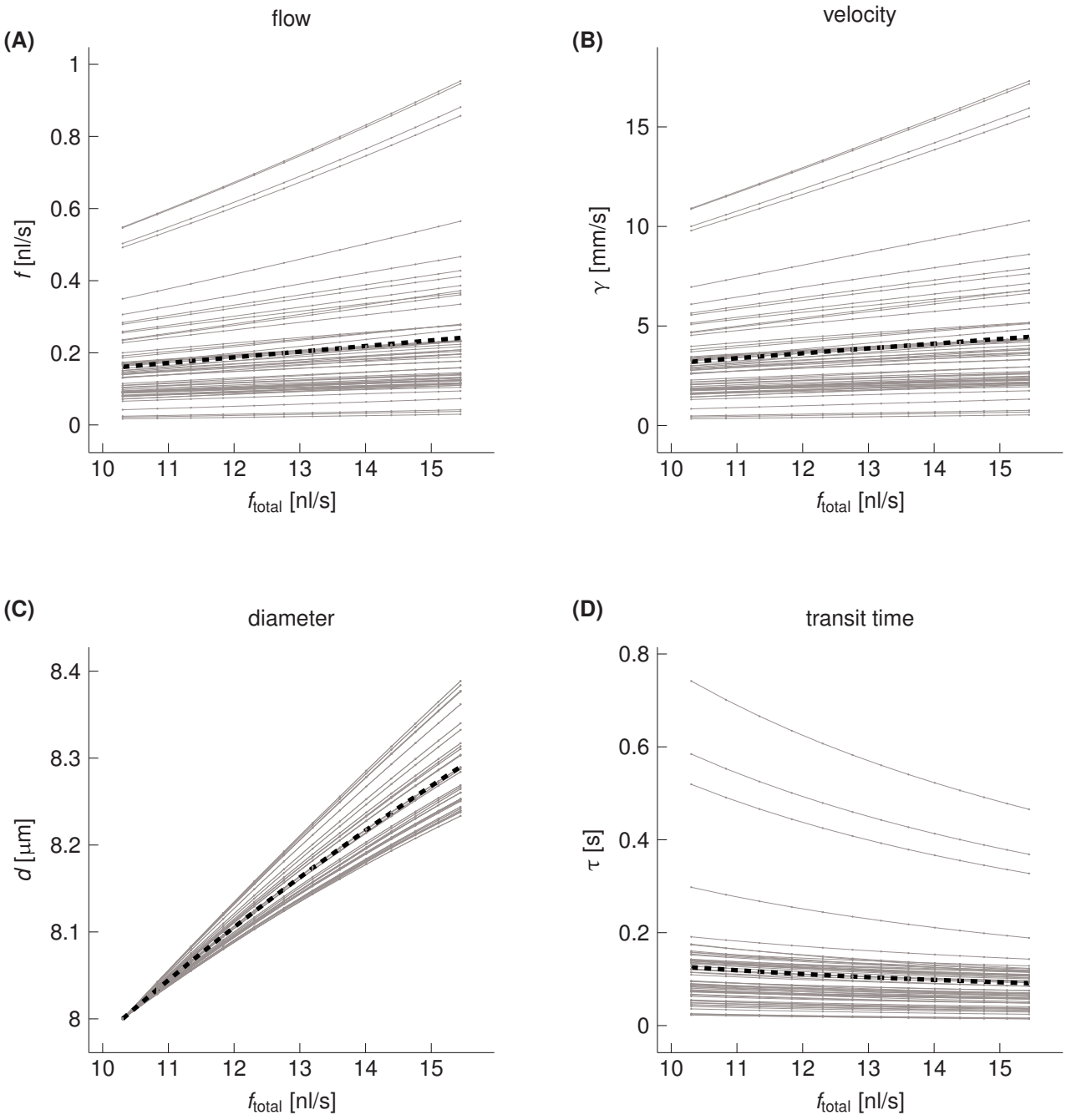

Figure 1: Behaviour of absolute **(A)**: capillary flow f, **(B)**: velocity γ, **(C)**: diameter d, and **(D)**: transit time τ of 64 individual capillaries (thin gray curves) against changes in total capillary flow f_{total}. Thick dashed curves are averages over all capillaries.

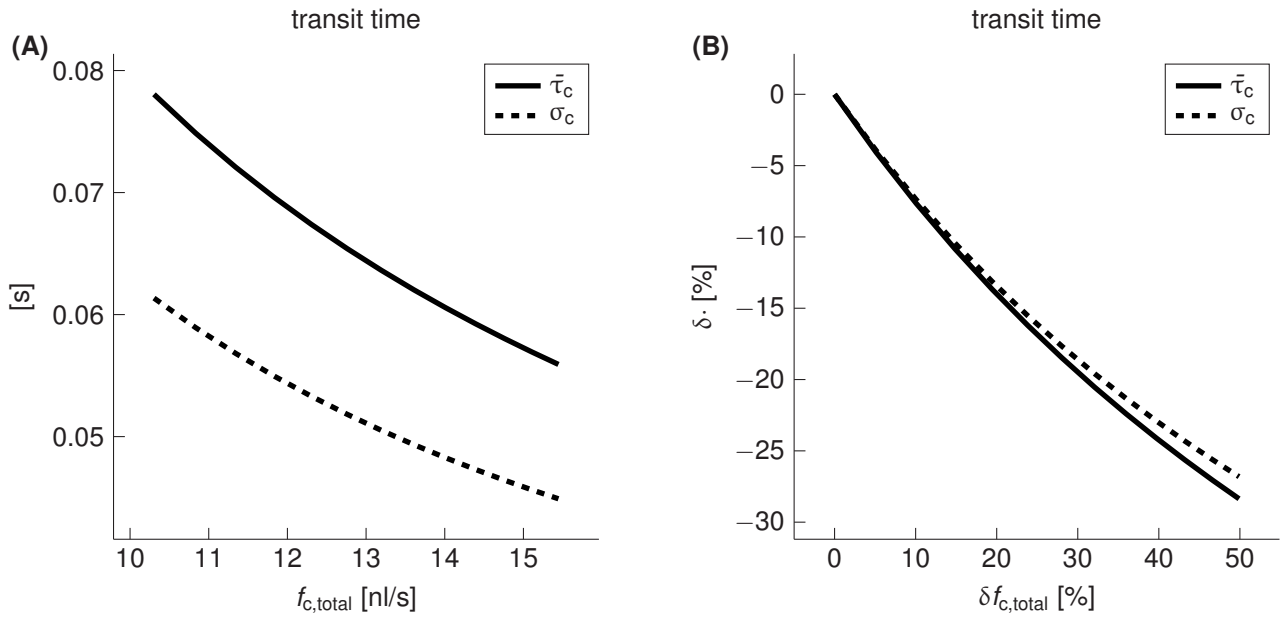

Figure 2: Traces of average capillary transit time ($\bar{\tau}_c$) and transit time standard deviation (σ_c). **(A)**: Quantities on absolute scales, **(B)**: relative changes in the quantities.

Model parameters

Table 1 and 2 show model parameters. The models are completely parameterized by these parameters. Note that baseline flow, baseline metabolism, and the oxygen conductance (E) are not defined in the tables. These parameters are part of lumped model parameters that appear after mathematical manipulation of the models' equations. Lumped parameters were computed from parameters in Table 1 and 2. For example, the baseline metabolism is part of a lumped model parameter that is computed from K_m, λ, and $p_{i,0}$.

Parameters values of the one-compartment model used in steady state simulations		
Parameter	Parameter value	Reference
$\bar{\tau}_c$ [s]	1.2	[9, 10, 11, 12]
λ [ml O_2/mL blood]	0.206	[13]
$p_{ac,0}$ [mmHg]	60	[14, 15]
$p_{cv,0}$ [mmHg]	35	[14, 15]
$p_{t,0}$ [mmHg]	25	[8, 15, 1]
p_{50} [mmHg]	36.0	[13]
h	2.60	[13]
K_m	0.001 \$	-
$\sigma_{c,0}$ [s]	0.94 ‡	[1]

Table 1: Parameters values of the one-compartment model used for simulation of steady state properties of the oxygen transport model. ‡ Corresponding to $\sigma_c/\bar{\tau}_c = 0.78$. \$ With this value the factor $p_t/(K_m + p_t)$ primarily prevents p_t from becoming negative while having a relatively small impact on the oxygen metabolism since the relative difference between m and m^{max} is less than 1% if $p_t > 0.1$ mmHg so $m \approx m^{\max}$.

Parameters values of the multi-compartment model used in modeling dynamical effects of capillary transit time heterogeneity		
Parameter	Parameter value	Reference
β	[1 4]	[16, 11]
$\bar{\tau}$ [s]	[0.5 4]	[9, 11, 12]
c_a	[0.5 0.9] $^{\diamond}$	[16, 11]
w_c	[0.4 0.5] †	[10]
w_t	[32 49] ‡	[10, 17]
λ [ml O_2/mL blood]	0.206 *	[13]
$p_{in,0}$ [mmHg]	77.9 *	[18]
$p_{ac,0}$ [mmHg]	[55 70]	[14, 15]
$p_{cv,0}$ [mmHg]	33.5 *	[18]
$p_{out,0}$ [mmHg]	33.5 *$\diamond$	[18]
$p_{t,0}$ [mmHg]	[20 30]	[8, 15, 1]
p_{50} [mmHg]	36.0 *	[13]
h	2.60 *	[13]
K_m	0.001 *\$	-
$\sigma_{c,0}$ [s]	[0.1 2]	[1]

Table 2: Parameters values of the multi-compartment model used in simulations of dynamics and for modeling the data set of Vazquez et al. [18]. Values marked with * were fixed, whereas intervals define the range of the prior distributions used in the analysis of the data set of [18]. The center values of the intervals were used in the simulations of dynamics. $\diamond$ Fractional contribution of the arteriolar compartment to the total resistance, the remaining resistance was equally distributed between the capillary and the venous compartment. $\dagger$ w_c Fractional capillary contribution to the total vascular volume, the remaining vascular volume was equally distributed between the arterial and the venous compartment. $\ddagger$ w_t Fraction of tissue volume to vascular volume. The interval corresponds to a tissue volume of 97%-98% of total volume. $\diamond$ To simplify, we assume negligible oxygen exchange between the venous compartment and tissue. \$ With this value the factor $p_t/(K_m + p_t)$ primarily prevents p_t from becoming negative while having a relatively small impact on the oxygen metabolism since the relative difference between m and m^{max} is less than 1% if $p_t > 0.1$ mmHg so $m \approx m^{\max}$.

Temporal dynamics of input variables

The temporal development of relative changes in input variables used in the analysis of the data set of Vasquez et al. [18] was modeled by the function $f(t)$. The function $f(t)$ increases from baseline towards a maximum value of θ_1 according to an asymmetrical sigmoid function [19] between times t_{min} and t_{max}, decreases exponentially towards a plateau value of θ_2 between times t_{max} and t_{end}, and finally decreases exponentially towards baseline value after time t_{end}. t_{min} and t_{end} are start and end times of the stimuli respectively, and t_{max} is the time of maximum response.

$$f(t) = \begin{cases} f_1(t) + 1, & t_{min} < t \leq t_{max} \\ f_2(t) + 1, & t_{max} < t \leq t_{end} \\ f_3(t) + 1, & t > t_{end}, \end{cases} \tag{3}$$

$$\begin{aligned} f_1(t) &= \theta_1 / \left[1 + g(t) \exp\{\theta_3 * (\theta_4 - t)\}\right. & (4) \\ &\quad \left. + \{1 - g(t)\} \exp\{\theta_5 * (\theta_4 - t)\}\right] & (5) \\ f_2(t) &= (s_1 - \theta_3) \exp\{\theta_6 * (t_{max} - t)\} + \theta_3 & (6) \\ f_3(t) &= s_2 \exp\{\theta_7 * (t_{end} - t)\}, & (7) \end{aligned}$$

where $s_1 = f(t_{max})$, and $s_2 = f(t_{end})$. $g(t) = 1/\left[1 + \exp\{-\gamma(\theta_4 - t)\}\right]$ where $\gamma = 2\theta_3\theta_5/|\theta_3 + \theta_5|$ and $\boldsymbol{\theta}$ holds model parameters.

References

[1] S. N. Jespersen and L. Østergaard. The roles of cerebral blood flow, capillary transit time heterogeneity, and oxygen tension in brain oxygenation and metabolism. *J. Cereb. Blood Flow Metab.*, 32(2):264–277, 2012.

[2] M. L. Schulte, J. D. Wood, and A. G. Hudetz. Cortical electrical stimulation alters erythrocyte perfusion pattern in the cerebral capillary network of the rat. *Brain Res.*, 963(1-2):81–92, 2003.

[3] B. Stefanovic, E. Hutchinson, V. Yakovleva, V. Schram, J. T. Russell, L. Belluscio, A. P. Koretsky, and A. C. Silva. Functional reactivity of cerebral capillaries. *J. Cereb. Blood Flow Metab.*, 28(5):961–972, 2008.

[4] A. Villringer, A. Them, U. Lindauer, K. Einhaupl, and U. Dirnagl. Capillary perfusion of the rat brain cortex. An in vivo confocal microscopy study. *Circ. Res.*, 75(1):55–62, 1994.

[5] A. G. Hudetz, B. B. Biswal, G. Feher, and J. P. Kampine. Effects of hypoxia and hypercapnia on capillary flow velocity in the rat cerebral cortex. *Microvasc. Res.*, 54(1):35–42, 1997.

[6] I. Krolo and A. G. Hudetz. Hypoxemia alters erythrocyte perfusion pattern in the cerebral capillary network. *Microvasc. Res.*, 59(1):72–79, 2000.

[7] D. A. Boas, S. R. Jones, A. Devor, T. J. Huppert, and A. M. Dale. A vascular anatomical network model of the spatio-temporal response to brain activation. *Neuroimage*, 40(3):1116–1129, 2008.

[8] R. B. Buxton. Interpreting oxygenation-based neuroimaging signals: the importance and the challenge of understanding brain oxygen metabolism. *Front Neuroenergetics*, 2:8, 2010.

[9] M. Ibaraki, H. Ito, E. Shimosegawa, H. Toyoshima, K. Ishigame, K. Takahashi, I. Kanno, and S. Miura. Cerebral vascular mean transit time in healthy humans: a comparative study with PET and dynamic susceptibility contrast-enhanced MRI. *J. Cereb. Blood Flow Metab.*, 27(2):404–413, 2007.

[10] B. Weber, A. L. Keller, J. Reichold, and N. K. Logothetis. The microvascular system of the striate and extrastriate visual cortex of the macaque. *Cereb. Cortex*, 18(10):2318–2330, Oct 2008.

[11] T. J. Huppert, M. S. Allen, S. G. Diamond, and D. A. Boas. Estimating cerebral oxygen metabolism from fMRI with a dynamic multicompartment Windkessel model. *Hum Brain Mapp*, 30(5):1548–1567, May 2009.

[12] V. E. Griffeth and R. B. Buxton. A theoretical framework for estimating cerebral oxygen metabolism changes using the calibrated-BOLD method: modeling the effects of blood volume distribution, hematocrit, oxygen extraction fraction, and tissue signal properties on the BOLD signal. *Neuroimage*, 58(1):198–212, 2011.

[13] Carl-Friedrich Cartheuser. Standard and pH-affected hemoglobin - O_2 binding curves of sprague-dawley rats under normal and shifted P_{50} conditions. *Comparative Biochemistry and Physiology Part A: Physiology*, 106(4):775–782, 1993.

[14] E. Vovenko. Distribution of oxygen tension on the surface of arterioles, capillaries and venules of brain cortex and in tissue in normoxia: an experimental study on rats. *Pflugers Arch.*, 437(4):617–623, Mar 1999.

[15] A. Devor, S. Sakadžić, P. A. Saisan, M. A. Yaseen, E. Roussakis, V. J. Srinivasan, S. A. Vinogradov, B. R. Rosen, R. B. Buxton, A. M. Dale, and D. A. Boas. "Overshoot" of O2 is required to maintain baseline tissue oxygenation at locations distal to blood vessels. *The Journal of Neuroscience*, 31(38):13676–13681, 2011.

[16] J. B. Mandeville, J. J. Marota, C. Ayata, G. Zaharchuk, M. A. Moskowitz, B. R. Rosen, and R. M. Weisskoff. Evidence of a cerebrovascular postarteriole windkessel with delayed compliance. *J. Cereb. Blood Flow Metab.*, 19(6):679–689, Jun 1999.

[17] J. Reichold, M. Stampanoni, A. Lena Keller, A. Buck, P. Jenny, and B. Weber. Vascular graph model to simulate the cerebral blood flow in realistic vascular networks. *J. Cereb. Blood Flow Metab.*, 29(8):1429–1443, Aug 2009.

[18] A. L. Vazquez, M. Fukuda, M. L. Tasker, K. Masamoto, and S. G. Kim. Changes in cerebral arterial, tissue and venous oxygenation with evoked neural stimulation: implications for hemoglobin-based functional neuroimaging. *J. Cereb. Blood Flow Metab.*, 30(2):428–439, Feb 2010.

[19] J. H. Ricketts and G. A. Head. A five-parameter logistic equation for investigating asymmetry of curvature in baroreflex studies. *Am. J. Physiol.*, 277(2 Pt 2):R441–454, Aug 1999.